Schizophrenia Bulletin vol. 35 no. 1 pp. 67–81, 2009
doi:10.1093/schbul/sbn133

Auditory Oddball Deficits in Schizophrenia: An Independent Component Analysis of the fMRI Multisite Function BIRN Study

Dae Il Kim[1,2], D.H. Mathalon[3], J.M. Ford[3], M. Mannell[2], J.A. Turner[4], G.G. Brown[5], A. Belger[6], R. Gollub[7], J. Lauriello[8], C. Wible[9], D. O'Leary[10], K. Lim[10], A. Toga[11], S.G. Potkin[4], F. Birn[4], and V.D. Calhoun[2,3,12]

[2]The Mind Research Network, 1101 Yale Boulevard NE, Albuquerque, NM 87131; [3]Department of Psychiatry, Yale University, New Haven, CT 06520; [4]Department of Psychiatry and Human Behavior, University of California Irvine, Irvine, CA 92697; [5]Department of Psychiatry, University of California San Diego, San Diego, CA 92161; [6]Brain Imaging and Analysis Center, Duke University Medical Center, Durham, NC 27710; [7]Neuroimaging Division, Department of Psychiatry, Massachusetts General Hospital, Charlestown, MA 02129; [8]Department of Psychiatry, University of New Mexico, Albuquerque, NM 87131; [9]Department of Radiology, Brigham Woman's Hospital, Boston, MA 02115; [10]Department of Psychiatry, University of Iowa, Iowa City, IA 52242; [11]Department of Neurology, University of California Los Angeles, LA 90095; [12]Department of Electrical and Computer Engineering, University of New Mexico, Albuquerque, NM 87131

Deficits in the connectivity between brain regions have been suggested to play a major role in the pathophysiology of schizophrenia. A functional magnetic resonance imaging (fMRI) analysis of schizophrenia was implemented using independent component analysis (ICA) to identify multiple temporally cohesive, spatially distributed regions of brain activity that represent functionally connected networks. We hypothesized that functional connectivity differences would be seen in auditory networks comprised of regions such as superior temporal gyrus as well as executive networks that consisted of frontal-parietal areas. Eight networks were found to be implicated in schizophrenia during the auditory oddball paradigm. These included a bilateral temporal network containing the superior and middle temporal gyrus; a default-mode network comprised of the posterior cingulate, precuneus, and middle frontal gyrus; and multiple dorsal lateral prefrontal cortex networks that constituted various levels of between-group differences. Highly task-related sensory networks were also found. These results indicate that patients with schizophrenia show functional connectivity differences in networks related to auditory processing, executive control, and baseline functional activity. Overall, these findings support the idea that the cognitive deficits associated with schizophrenia are widespread and that a functional connectivity approach can help elucidate the neural correlates of this disorder.

Key words: fMRI/DLPFC/schizophrenia/default-mode/independent component analysis/auditory oddball

Introduction

Schizophrenia is a mental disorder with an unknown etiology and pathophysiology. It is often associated with a number of neurobiological deficits with one of the most consistent markers found in event-related potential (ERP) recordings of auditory target detection tasks.[1] For example, the amplitude of the P300 potential elicited by decision making is reduced in patients with schizophrenia. In the context of an auditory target detection task, the P300 is elicited by target detection of infrequent auditory stimuli. Intracranial recordings during the performance of this task in neurosurgery patients indicate multiple distributed neural generators of the P300, including ventrolateral prefrontal, inferior temporal, perirhinal cortices, superior temporal sulci, posterior parietal association cortices, and hippocampus.[2,3] However, intracranial recordings are not available for schizophrenia patients; thus, attempts to spatially localize the deficits for this population have led to functional magnetic resonance imaging (fMRI) studies of similar tasks.

A common method of analyzing fMRI datasets relies on the general linear model (GLM), which is an excellent tool for finding regions that are engaged during a particular task assignment. However, the GLM cannot identify brain regions that are functionally connected to one another. The substantial base of neuroimaging literature that deals with schizophrenia suggests that its cognitive deficits are not localized to a single region of the brain but are representative of a more widespread cognitive dysfunction.[4] Previous studies have also shown reduced temporal-frontal connectivity in this population[5,6] as well as an overall group difference in the effective connectivity

[1]To whom correspondence should be addressed; The Mind Research Network Institute, Albuquerque, NM 87131; tel: 646-675-9193, e-mail: dkim@mrn.org.

between predefined regions of interest (ROIs).[7] The aberrant P300 in schizophrenia patients might also be the result of dysfunctional connectivity between its relevant brain regions, resulting in its significantly reduced amplitude. Thus, the study of schizophrenia could benefit from a functional connectivity approach that is not limited to previously determined ROIs.

Independent component analysis (ICA) is one such method because it is capable of revealing hidden factors that underlie sets of random variables, measurements, or signals. ICA assumes that fMRI data are linear mixtures of independent source signals and attempts to extract maximally independent signals and their mixing coefficients. The driving principle behind ICA is that these independent source signals represent coherent groupings of fMRI activations, often referred to as component maps, that imply a representation of a functionally connected network.[8] Because ICA is a data-driven approach, the functional networks are generated without any assumptions about the shape of the fMRI time courses and thus can capture coherent activity that does not track strongly with a task.

Based on previous research, we hypothesized that the fMRI data collected during an auditory oddball paradigm in patients with schizophrenia would show significant differences from control subjects in networks that included the anterior cingulate cortex (ACC), dorsal lateral prefrontal cortex (DLPFC), inferior parietal regions, and cerebellum.[9,10] A previous study utilizing a similar oddball paradigm and ICA showed significant differences in the default-mode network (DMN)[11] as well, a set of regions hypothesized to represent a baseline state of activity. There is also a strong consistency in the spatial patterns of activation for the functional networks found using ICA in fMRI.[12,13] Between these independent networks, common brain regions of activation are often found, and we were interested in the degree with which they overlap with one another. Recent studies have shown that networks such as the DMN might be actually composed of multiple subsystems sharing common regions such as the posterior cingulate.[14] In this context, the brain regions involved in auditory target detection could consist of multiple brain networks sharing a similar ROI. This particular region could then act as a possible ''switching'' station to relay its information to higher order systems for further processing.

To pursue these hypotheses, we acquired data from a multisite study called the functional biomedical informatics research network (fBIRN) collaboration. The multisite project consists of multiple research institutions that have participated in the acquisition of fMRI data from patients with schizophrenia.[15] Across these sites, fMRI datasets were collected from stably medicated patients diagnosed with a chronic form of schizophrenia ($n = 66$) and demographically matched healthy controls ($n = 71$). Participants performed a 2-tone auditory oddball paradigm auditory while inside the scanner for 4 experimental sessions. They were instructed to listen for an oddball tone (deviants) and to respond with a button press while ignoring standard tones.

Methods

Participants

All sites received local Institutional Review Board approval for this study, and all participants provided written informed consent. Male and female healthy comparison subjects ($n = 71$; 43 men) and schizophrenic/schizoaffective adults ($n = 66$; 43 men) between the ages of 18 and 70 years were recruited. Within the patient group, 60 participants were right-handed, and 6 were left-handed. For controls, 64 participants were right-handed, 3 were left-handed, and 4 were both. All subjects had normal hearing (no more than a 25 db loss in either ear) and were able to perform the task. Control subjects were excluded if they had a current or past history of a major neurological, psychiatric, medical illness; previous head injury; substance or alcohol dependence; IQ less than 75 (as measured by the North American Adult Reading Test [NAART]); if they were using migraine treatments; or if a first-degree family member had a diagnosis of a psychotic illness.

Patients meeting the Structured Clinical Interview *Diagnostic and Statistical Manual of Mental Disorders, Fourth Edition (DSM-IV),* criteria for schizophrenia or schizoaffective disorder participated in the study; schizophreniform subjects were excluded. Diagnosis for schizoaffective disorder was determined by meeting criteria A for schizophrenia in the *DSM-IV*, which includes all the relevant axes and that a significant portion of their illness includes identifiable depression or mania. Moreover, their psychotic symptoms must exist for at least 2 weeks without any notable mood abnormality fueling their psychosis. The decision to use both schizoaffective and schizophrenia subjects was partially due to the lack of a distinct pathology in the literature that underlies one versus the other. Symptom scores were determined by using the Schedule for the Assessment of Positive Symptoms (SAPS)[16] and Negative Symptoms[17] assessment measures and are listed in table 1. Subjects were excluded if they had a current major medical illness, previous head injury or prolonged unconsciousness, or substance and/or alcohol dependence. Patients were also excluded if they currently had an IQ less than 75 as measured by the NAART, migraine treatments, significant extrapyramidal symptoms, or tardive dyskinesia (measured by the Global section of the abnormal involuntary movement scale). Subjects were required to be clinically stable with no significant changes in their psychotropic medications in the previous 2 months. However, a detailed history of their medication status was not available for this study.

Table 1. Demographic Information, NART IQ Measurements, and Symptom Score Assessment Using SANS and SAPS for Patients With Schizophrenia Are Listed Here

Demographics	Schizophrenia (Mean/SD)	Controls (Mean/SD)	Statistics (t)/P Value
Sex (M/F)	43/23	43/28	
Age (y)	37.4 (11.7)	35.3 (10.6)	$t_{135} = 1.65/.01$
Education (y)	13.6 (1.9)	15.7 (2.0)	$t_{127} = 6.19/.0001$
Maternal education	14.5 (11.9)	14.4 (2.6)	$t_{122} = 0.04/.97$
Paternal education	15.3 (2.0)	15.0 (3.3)	$t_{122} = 0.26/.8$
NAART			
Verbal IQ	103.83 (11.04)	110.67 (8.68)	$t_{125} = 3.91/.0002$
Performance IQ	107.77 (5.38)	110.89 (4.09)	$t_{125} = 3.72/.0003$
Full-scale IQ	106.00 (9.68)	112.00 (7.60)	$t_{125} = 3.91/.0001$
Schizophrenia symptom scores			
SAPS ($n = 62$)	Mean (SD)	SANS ($n = 65$)	Mean(SD)
Hallucinations	1.89 (1.74)	Affect	1.71 (1.35)
Delusions	2.31 (1.57)	Alogia	1.14 (1.21)
Bizarre behavior	0.84 (1.13)	Avolition	2.29 (1.32)
Thought disorder	1.03 (1.21)	Anhedonia	2.34 (1.36)
		Attention	1.28 (1.19)

Note: NAART, North American Adult Reading Test; SANS, Schedule for the Assessment of Negative Symptoms; SAPS, Schedule for the Assessment of Positive Symptoms. Significant group differences were seen for years of education and NAART IQ measures.

The 2 groups did not differ with regard to age (patients: 37.4 years [SD = 11.7 years], controls: 35.3 years [SD = 10.6 years], $t_{135} = 1.65$, $P < .10$). Significant differences were found with regard to the number of years of education (patients: 13.6 years [SD = 1.9 years], controls: 15.7 years [SD = 2.0 years], $t_{127} = 6.19$, $P < .0001$), but no significant differences were found for paternal (patients-fathers: 15.3 years [SD = 11.7 years], controls-fathers: 15.0 years [SD = 3.3 years], $t_{122} = 0.26$, $P < .80$) or maternal education (patients-mothers: 14.5 years [SD = 11.9 years], controls-mothers: 14.4 years [SD = 2.6 years], $t_{122} = 0.04$, $P < .97$).

Auditory Oddball Paradigm

The auditory oddball paradigm used in this study is a 2-tone oddball task where the participant is presented with a continuous sequence of 2 discrete simuli (''deviants'' and ''standards''). Standards are physically identical auditory stimuli that appear in 95% of the trials. Deviants, or oddball tones, are higher in pitch than standards and occur in only 5% of the trials. The task consists of 2 practice runs and 4 experimental runs, each having a duration of 280 seconds (4.67 minutes). Each run consists of multiple presentations of a standard tone (1000 Hz) and an oddball/deviant tone (1200 Hz) presented binaurally. Each subject adjusted the volume of a test stimulus to the left and right ears so that it could be heard comfortably over the noise of the scanner during an echo-planar imaging (EPI) scan. Throughout the duration of the auditory stimuli, participants are asked to fixate on a black cross centered on a gray screen. They are instructed to press the first button on their right hand in response to a deviant tone and to do nothing in response to standard tones. The task begins with a fixation block that lasts for 15 seconds. This is then followed by the presentation of the standard tones (interstimulus interval [ISI] = 500 milliseconds, duration = 100 milliseconds). Every 6–15 seconds, the oddball tone is presented (ISI = 500 milliseconds, duration = 100 milliseconds). The task is concluded with another 15-second block of silence.

Imaging Parameters

Pulse sequence parameters for all sites were matched as closely as possible based on preliminary studies conducted by the fBIRN group[15,18] (orientation: anterior commissure–posterior commissure line, number of slices: 27, slice thickness = 4 mm, time to repeat = 2000 milliseconds, time to echo = 30 milliseconds (3T)/40 milliseconds (1.5T), field of view = 22 cm, matrix 64 × 64, flip angle = 90°, voxel dimensions = 3.4375 × 3.4375 ×4 mm). Duke University utilized a spiral echo sequence while all other sites employed a single-shot EPI sequence (table 2).

Data Analysis: Preprocessing

Datasets were preprocessed using SPM5 (http://www.fil.ion.ucl.ac.uk/spm/software/spm5/). Images were realigned using INRIalign—a motion correction algorithm unbiased by local signal changes.[19,20] A slice-timing correction was performed on the fMRI data after realignment to account for possible errors related to the temporal variability in the acquisition of the fMRI datasets. Data were spatially normalized[21] into the standard Montreal Neurological Institute (MNI) space using an echo planar imaging template found in SPM5 and slightly subsampled to 3 mm^3, resulting in 53 × 63 × 46 voxels. Finally, data were spatially smoothed with a 9 × 9 ×9 mm^3 full width at half-maximum Gaussian kernel.

Table 2. Imaging Parameters and Number of Participants Varied Across Scanner Sites

Institution	Scanner	Tesla	Sequence	Patients	Controls
Duke/UNC	GE Nvi Lx	4.0T	Spiral	9	11
Brigham and Women's Hospital	GE	3.0T	EPI	4	5
Massachusetts General Hospital	Siemens Trio	3.0T	EPI	5	0
University of California—Los Angeles	Siemens Allegra	3.0T	EPI	7	10
University of California—Irvine	Marconi Eclipse	1.5T	EPI	6	9
University of New Mexico	Siemens Trio	1.5T	EPI	13	13
University of Iowa	Siemens Trio	3.0T	EPI	8	10
University of Minnesota	Siemens Trio	3.0T	EPI	14	13

Most scanners utilized an echo-planar imaging sequence for their functional magnetic resonance imaging blood–oxygen–level–dependent sequences with the exception of Duke/UNC.

Independent Component Analysis

General Overview. Following Calhoun et al,[22] the ICA was performed using the GIFT toolbox, version 1.3c (http://icatb.sourceforge.net). Here, we describe a general overview of the ICA analyses. For a full explanation of the ICA algorithm and its theoretical constructs, we refer the reader to these relevant articles.[22–24] Using a modified minimum description length (MDL) algorithm,[25] the optimal number that ICA used to split the fMRI datasets into a final set of spatially independent components was determined to be 25. Because group ICA requires that all subjects are analyzed at once, a method for data compression using principal component analysis (PCA) allowed the datasets to be loaded into memory at one time.[22] There are 2 PCA data reduction steps: In the first step, data from each subject and each session were reduced from 140 (the number of timepoints within the experiment) to 25 dimensions. We have found that the number of dimensions for the first data reduction step does not significantly affect the results as long as this number is not much smaller than the number specified by the MDL algorithm.[22,26] In the second step, the compressed datasets for each subject and session are then concatenated with one another and reduced again to the final 25 components found from the MDL algorithm. A group spatial ICA is then performed using the infomax algorithm.[27] It is important to note that group ICA is performed on all the subjects at once, and significant between-group differences are determined by a second-level analysis of the ICA results.

The resulting output is an independent component spatial map and a single associated ICA timecourse for every component, subject, and session. Thus, for our subject pool of 137 subjects, we produced 13,700 (137 subjects × 4 sessions × 25 components = 13,700) independent component spatial maps, each associated with a single ICA timecourse. The ICA timecourse and their spatial maps are then calibrated using z scores.[13,28] This calibration step is important because the units are not constrained by any specific measure and are arbitrary. What is important is the relative change within these units so that a large signal change within the ICA timecourse would be represented by a strong deviation from the mean or a high z score. Likewise, a high z score within the spatial maps represents a stronger representation of the ICA timecourse as well. These spatial maps and timecourses are then subjected to a second-level analysis to determine which components are task related and are not representative of noise/artifacts. The second-level analysis can be split into 2 parts, the analysis of the ICA timecourses and the analysis of the independent spatial component maps. They are discussed in more detail below, and an overview of the entire analysis can be seen in figure 1.

Statistical Analysis of Component Timecourses. A regression was performed on the ICA component timecourses with the GLM design matrix taken from SPM5. This design matrix represents a combination of the experimental onsets convolved with a canonical hemodynamic response function. This resulted in a set of beta weights for every experimental regressor (deviants, standards, and temporal derivatives) associated with a particular subject and component. The resulting beta weights from the regression represent the degree to which the component was modulated by the task relative to the fixation baseline. In other words, the regression of the timecourses to the design matrix is an attempt to answer the question of how significant a component is with respect to specific aspects of the experiment (and is directly analogous to the GLM fit that is typically performed on each voxel of the preprocessed fMRI data, however in this case it is performed on the ICA timecourse). Thus, a high beta weight can be considered to represent a large task-related modulation of a component for a given regressor.

Beta weights associated with the deviants and deviants minus standards condition were chosen for further statistical analysis. In the context of ICA, we regressed this condition to obtain beta weights that represent the degree to which this condition modulated our ICA timecourse. The key factor in determining between-group differences in ICA lies within the analysis of these resulting beta

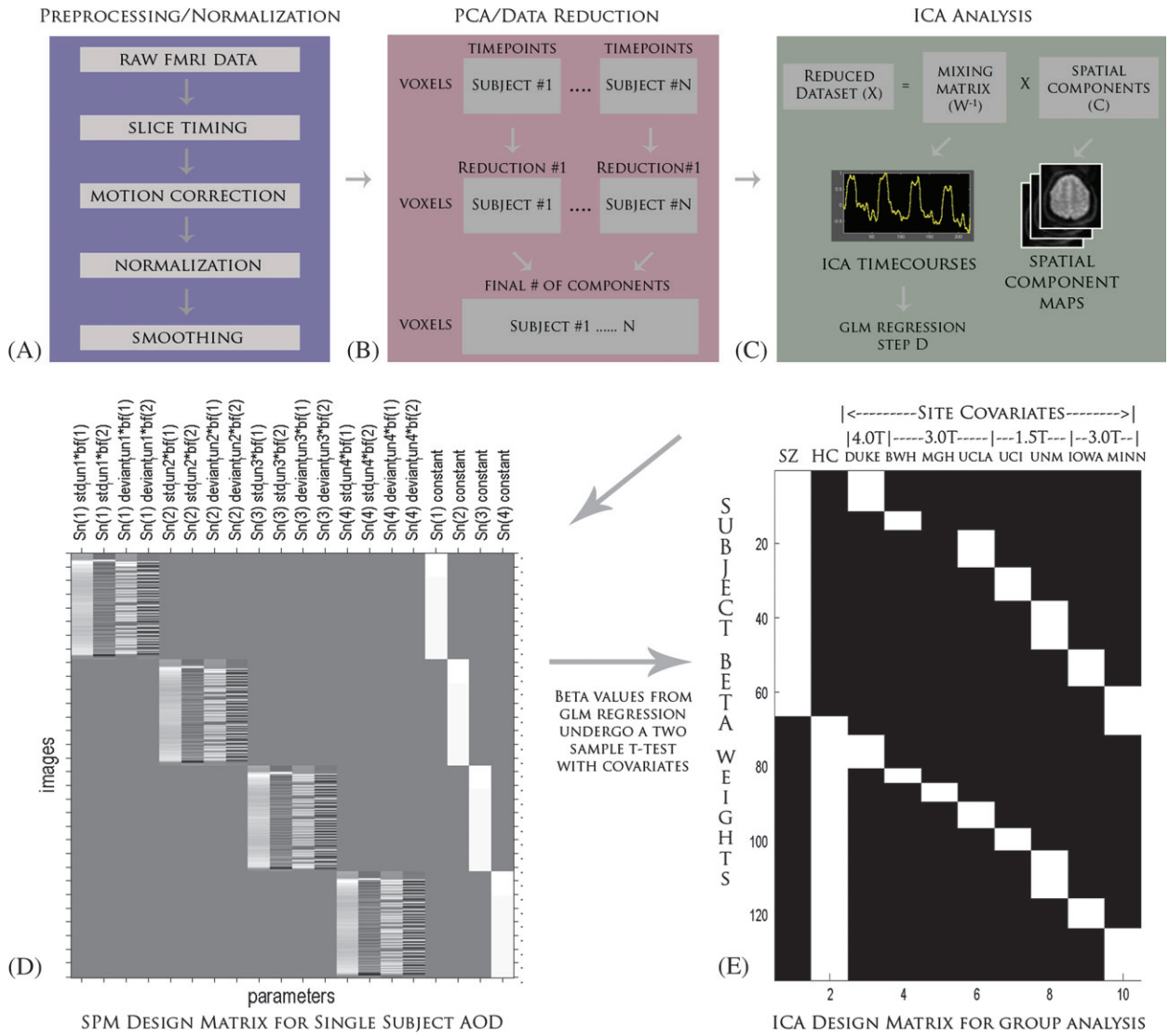

Fig. 1. A) An Overview of the Entire Independent Component Analysis (ICA) Starting From the Raw Functional Magnetic Resonance Imaging datasets. The datasets must first be preprocessed before entering an ICA, and the steps used for our specific analysis are listed here. B) Once the datasets are preprocessed, they are reduced using PCA. Each subject's dataset is reduced in the time dimension to a parameter specified during the analysis. These datasets are then concatenated together across time and reduced further to a final number of dimensions, which is equivalent to the final number of components. C) ICA splits this reduced dataset (X) into a mixing matrix (W^{-1}) that represents the ICA timecourses and a set of associated spatial components (C). D) The ICA timecourses undergo a regression with the SPM design matrix to create a set of betas that will be used to determine task relevance and group differences. E) The ICA design matrix used here performs a 2-sample *t* test with covariates for site and scanner strength.

weights. By performing a 2-sample *t* test on these beta weights, a resulting *P* value can be generated that depicts a statistical measure of difference between patients and controls for that particular regressor. In essence, this procedure attempts to determine how differently the 2 groups modulate their particular ICA networks in response to these two conditions.

Event-related averages were calculated for each component's timecourse for patients and controls separately during the onset of the deviant stimuli. Timecourses were overlaid for both groups that extended for 5 TRs or 10 seconds following stimulus onset. The event-related averages can be considered to depict the activation of the ICA timecourse, reflecting the activation for a given component and its associated brain regions. A stronger amplitude for one group versus another suggests that this timecourse is modulated more strongly than the other group, and we can determine the direction of group differences by observing these averaged timecourses. Another perspective is that the *z* scores associated with the voxels for an independent component spatial map are directly proportional to the amplitude of its associated ICA timecourse. Thus, one can visualize the areas of high activation found from the spatial component

maps as a strong representation of that component's ICA timecourse.

Statistical Analysis of Spatial Maps. The spatial maps generated by ICA were averaged together across the 4 scans sessions resulting in 25 independent component spatial maps for every subject. These spatial maps, representing the regions of the brain that are related to the ICA timecourse, were then calibrated using z scores. Each voxel within a component's spatial map retains a z score. As stated before, regions containing higher z scores reflect a greater contribution of that area to its associated timecourse. To determine the overall group effect of ICA for a given component, a random-effects analysis of the raw spatial maps, across all subjects, was performed in SPM5 for each individual component using a false discovery rate (FDR) correction (FDR, $P < 1 \times 10^{-12}$).[29] The final maps generated from this statistical analysis were used to determine a component's relevant brain regions. It is important to note that the statistical analyses of the spatial maps do not determine whether a given component is task related. It merely represents a statistical visualization of the relevant regions for that component under a specified threshold (ie, $P < 1 \times 10^{-12}$, FDR corrected).

Quality Assurance and Site Differences. We attempted to remove the effect of site differences by creating a regression model that included covariates accounting for each site. We then applied this regression to the beta weights that were originally generated from the regression of the ICA timecourse with the GLM design matrix. As mentioned before, the determination of between-group differences (P values for a specific regressor) was initially generated by performing a 2-sample t test on the resulting beta weights. The difference here is in the modification of these beta weights for site differences. The t tests were then performed again on the resulting site-adjusted beta weights and then converted into P values with an FDR correction. Our results and discussion deal only with the P values that were calculated using the site-adjusted beta weights.

We also examined the site differences directly by averaging the beta weights for our deviants versus standard tone condition across all subjects by site and scanner strength for each component. This allowed us to visualize the differences between these factors and their contributions for a given component. We were concerned with the directionality of the averaged beta weights and whether certain sites were outliers in the analysis and thus plotted these for 5 components that we found to be significant to our analyses (figure 2).

Component Selection. We decided upon 3 phases for finding components that were of interest for further analysis. Our first criterion was that components that showed a relatively high spatial correlation with white matter and cerebral spinal fluid (CSF) were most likely artifactual and could be discarded from the analysis. To accomplish this, we correlated each ICA component spatial map with prior probabilistic maps of white matter and CSF within a standardized brain space provided by MNI templates in SPM5. This process plays particularly well to the strengths of ICA, which is known for its ability to find noise-related components that represent head motion, physiological noise, eyeball movement, and other signal artifacts. Components that scored a higher spatial correlation value ($r^2 = 0.025$) with CSF and ($r^2 = 0.01$) with white matter maps were not considered to be meaningful activations and discarded in a manner similar to a previous study by Stevens et al.[23]

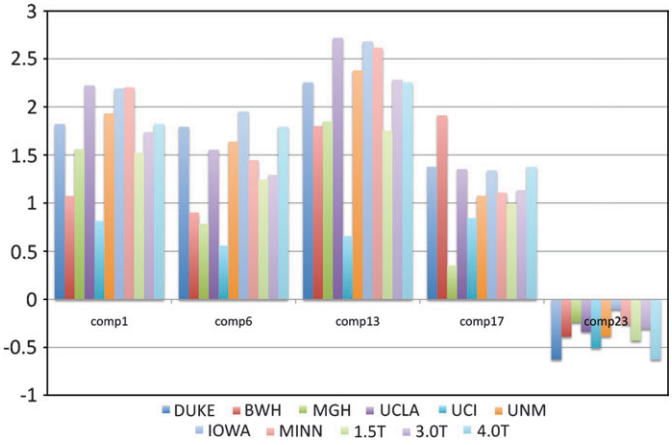

Fig. 2. Site Differences by Averaged Beta Weights for 5 Components. Directionality of the beta weights suggests a similar contribution for each site across components.

Those that survived this first phase were then subjected to our second criterion of experimental task relevance. In other words, we were interested in components that were highly correlated with the experimental design, and we attempted to determine this by using a GLM approach similar to one seen in SPM5. The difference lies in the timecourses that are being regressed. In the standard GLM approach, every voxel within the brain is subjected to the GLM design matrix, and a set of betas are generated for each voxel as well. In this ICA analysis, the ICA timecourse is regressed rather than the voxel timecourse and the betas or coefficients generated from this analysis represent how strongly the experimental design modulates the ICA timecourse. For our purposes, the beta weights associated with the deviants conditions for each component underwent a 1-sample t test ($P < .05$, FDR corrected) for patients and controls separately. If this distribution was significant for either controls or patients, it suggested that there was a meaningful relationship between the experimental task and the ICA timecourse that was generated. If a component failed to show a significant relationship for this

condition, it was considered to be nontask related and discarded.

Our third and final criterion consisted of determining whether the distribution of these beta weights for each group showed between-group significance. A 2-sample t test $P < .05$ (FDR corrected) was used to determine significant group differences for the deviants condition and a contrast condition (ie, deviants minus standards). Those that passed that final criterion were considered relevant and kept for further analysis with the exception of 2 components (C13, C23) that passed the first 2 criteria but not the third. Their inclusion in our discussion was due to the fact that C23 reflected a spatial activation pattern that was similar to regions of the default mode while C13 engaged primary auditory regions that are highly correlated in auditory tasks. (table 3).

Results

Behavioral Findings

No significant differences between patients and healthy controls were found in the percentage of correct responses (patients = 91.6%, SD = 7.5%, controls = 93.6%, SD = 7.5%, $t_{135} = 1.54$, $P < .13$) and mean reaction time to the deviants (patients = 468.2 milliseconds, SD = 107.0 milliseconds, controls = 438.1 milliseconds, SD = 104.3 milliseconds, $t_{135} = 1.66$, $P < .10$).

Between-Group Differences

Eight components were found that passed our selection criteria, and these were components 1, 3, 6, 8, 17, 19, 22, and 25 (C1, C3, C6, C8, C17, C19, C22, and C25, respectively; figure 3). Many of the components found to be relevant contained prefrontal regions of the brain, which often overlapped with areas such as the ACC and DLPFC. The most significant between-group difference was seen in C6 ($P < .0001$, table 4) that displayed robust activation within the ACC and DLPFC as well as areas within the thalamus and insula. The event-related average for this component showed that controls exhibited a much stronger positive modulation of this network than patients, which most likely accounted for the significant group difference. Another component that showed prefrontal activation was C17, which activated left DLPFC along with large areas of the inferior and superior parietal lobules. Similar to the event-related average for C6, this component showed a stronger positive activation for controls than patients but with a slightly earlier positive modulation of this signal for patients. The component that depicted bilateral DLPFC activation was C19 along with regions within the superior parietal and paracentral lobules. The event-related average for this component shows a similar shape to the event-related average for C6 but with a smaller difference in the magnitude of the positive signal change between patients and controls. Overall, these 3 components seem to occupy and overlap to various degrees within the prefrontal regions of the brain, with C6 heavily represented within that area and C17 distinguished more strongly by its activity within parietal areas.

A component that seems to delineate the visual sensory system was seen in C25. This component contained regions with the medial occipital lobe and was considered to represent activation within the primary visual regions of the brain. The event-related average for this component shows a stronger positive modulation of this signal for controls than patients, suggesting an interesting pattern of hypoactivity for patients in response to a deviant auditory stimulus. A component was also found that implicated regions mainly within the cerebellum in C1, overlapping to a small degree with C25 in areas such as the middle occipital gyrus. For this component's event-related average, controls again showed a stronger

Table 3. Components That Show Significant Between-Group Differences and Their Relevant *P* Values When Regressed With the Deviants Condition

	Deviants	Deviants (1-Sample t test)		Deviants Vs Standards	Deviants Vs Standards (1-Sample t test)	
Components	2-Sample t Test	Controls	Patients	2-Sample t Test	Controls	Patients
1	0.0018	0.0000	0.0000	0.0033	0.0000	0.0000
3	0.0356	0.0000	0.0116	0.0377	0.0008	0.1234
6	0.0001	0.0000	0.0000	0.0001	0.0000	0.0000
8	0.0104	0.0001	0.1759	0.0091	0.0002	0.2279
13	0.7624	0.0000	0.0000	0.6531	0.0000	0.0000
17	0.0019	0.0000	0.0000	0.0025	0.0000	0.0000
19	0.0035	0.0000	0.0000	0.0035	0.0000	0.0000
22	0.0018	0.0033	0.1388	0.0007	0.0000	0.6903
23	0.9465	0.0058	0.0020	0.8123	0.0924	0.0256
25	0.0406	0.0000	0.0000	0.0339	0.0000	0.0000

Components that showed 1-sample significance with the task for either controls or patients were allowed to undergo a 2-sample t test. Those components that passed a false discovery rate–corrected $P < .05$ were pursued for further analysis.

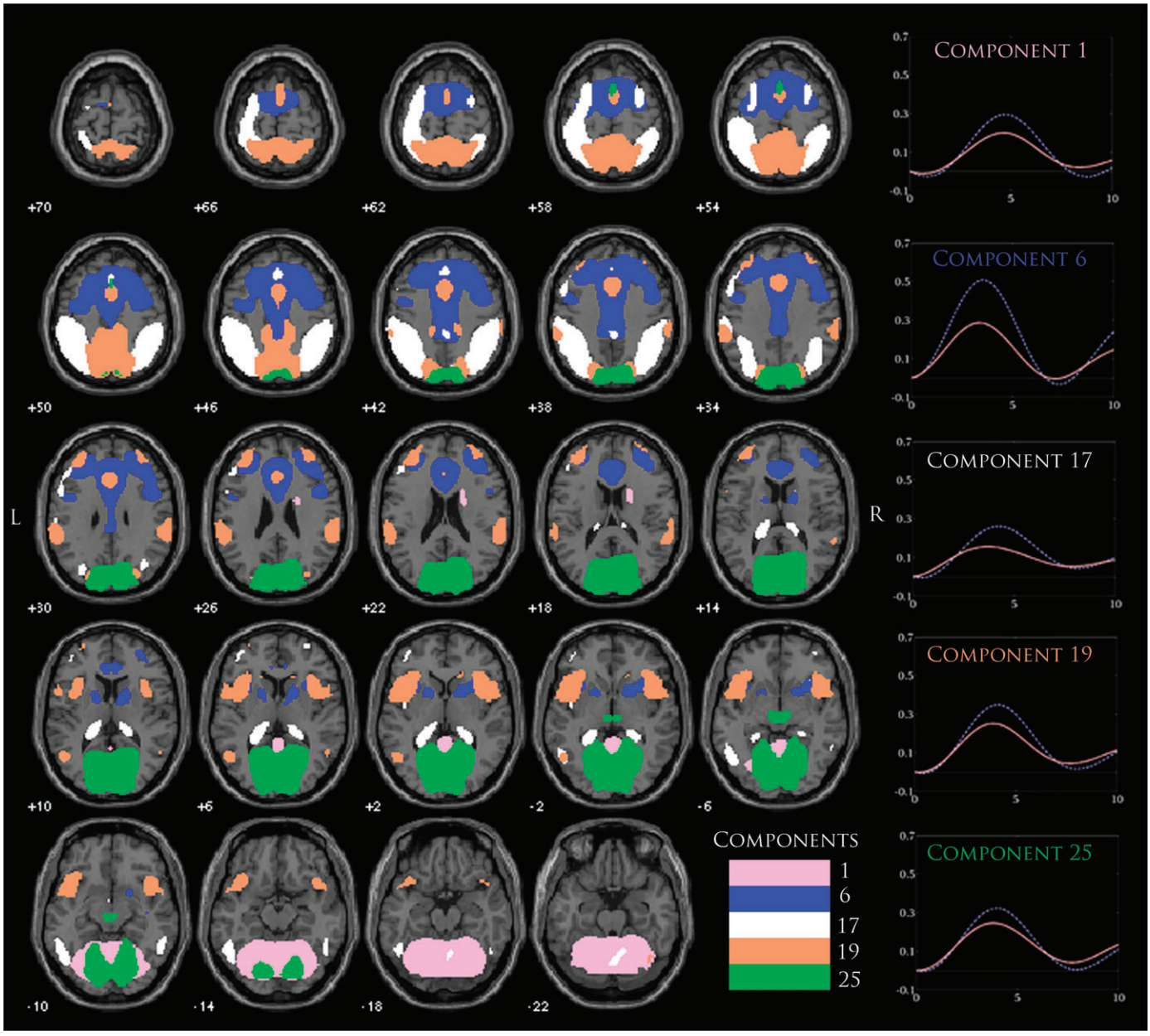

Fig. 3. An Overlay of 5 components (C1, C6, C17, C19, and C25) Thresholded at False Discovery Rate $P < 1.0 \times 10^{-10}$. Component maps were generated using a 1-sample random-effects analysis via the SPM5 toolbox. Event-related averages for each component are plotted on the right with separate timecoures for patients (red) and controls (blue dots). Other significant components (C3, C8, and C22) are shown in more detail in later figures.

positive modulation than patients, but unlike other components its peak activation was seen 5 seconds after the onset for both groups versus the usual 3–4 seconds for almost every other component.

We hypothesized that at least one component would show differences in regions within the auditory cortex based on previous schizophrenia research and due to the auditory nature of the task.[9,30] The components with significant group differences that engaged auditory regions within the brain were C3 and C8, which showed activation within bilateral middle and superior temporal gyri. Another component, C13, exhibited similar regions that were highly task correlated but was not found to show significant between-group differences. Considering that auditory processing could significantly differ for patients with schizophrenia, we were interested in the overlap of these components and the relationship between their respective ICA timecourses. To accomplish this, their respective spatial maps were overlaid together on a separate figure (figure 4). Regions colored in red represented an overlap between networks. The majority of the overlap between these 3 components seems to reside

Table 4. The Top 5 Brain Regions Within Each Component That Show the Highest Significance Based Off of a Random-Effects 1-Sample *t* Test Analysis in SPM are shown here

Component 1—Talairach Regions	Brodmann Areas	R/L (cm^3)	Maximum *t* Values (R/L)
Culmen		12.3/12.1	28.5 (–30, –53, –18)/31.7 (12, –67, –9)
Declive		7.9/8.0	27.7 (–27, –56, –17)/30.9 (18, –62, –12)
Declive of vermis		0.3/0.4	27.5 (0, –74, –14)/30.1 (3, –73, –11)
Fusiform gyrus	19, 37, 20	4.8/3.6	24.1 (–21, –59, –10)/29.4 (21, –62, –10)
Lingual gyrus	18, 19	8.5/8.3	27.6 (–6, –73, –6)/29.3 (6, –73, –6)
Component 3			
Middle temporal gyrus	21, 22, 39, 19, 37	20.0/21.2	32.6 (–56, –29, –6)/27.3(59, –46, 5)
Superior temporal gyrus	22 39, 21, 13, 42, 41, 38	19.5/18.7	25.5 (–53, –46, 13)/28.6 (59, –43, 8)
Subgyral	20, 21	7.4/6.9	27.9 (–48, –27, –9)/20.7 (48, –41, 5)
Supramarginal gyrus	40	6.1/4.2	23.2 (–56, –46, 22)/26.4(59, –54, 22)
Inferior temporal gyrus	21 20	1.2/0.1	21.5 (–56, –12, –15)/9.9 (56, –15, –17)
Component 6			
Medial frontal gyrus	32 6, 8, 9	13.2/13.4	32.3 (0, 11, 44)/32.7 (3, 8, 44)
Cingulate gyrus	32 24, 31, 23	19.8/16.5	30.3 (–3, 17, 41)/32.1(3, 11, 41)
Anterior cingulate	24 32, 33	5.3/5.7	29.4 (–6, 24, 24)/28.1(6, 30, 21)
Superior frontal gyrus	6 8, 9, 10	17.7/13.1	28.4 (–3, 8, 49)/26.5(3, 8, 49)
Middle frontal gyrus	10, 9, 6, 8, 46	27.7/15.8	23.8 (–33, 36, 29)/21.0 (30, 36, 29)
Component 8			
Superior temporal gyrus	38, 13, 22, 21	10.3/9.3	31.6 (–45, 8, –16)/33.6(42, 5, –15)
Subgyral	21, 20	5.8/6.8	28.0 (–45, 5, –18)/32.1 (45, 2, –15)
Middle temporal gyrus	21, 38	4.5/4.0	27.5 (–48, 5, –15)/28.8(48, 5, –15)
Extranuclear	13	1.6/3.2	20.6 (–39, 2, –10)/27.8 (42, 5, –10)
Inferior frontal gyrus	47, 13, 11	6.7/5.5	26.1 (–42, 23, –14)/27.4 (42, 17, –13)
Component 13			
Superior temporal gyrus	22, 13, 41, 42, 21, 38	20.7/20.2	40.3 (–50, –14, 9)/35.5 (48, –20, 9)
Insula	13, 40, 41, 47	15.9/17.3	36.4 (–4, –14, 9)/34.8 (45, –14, 6)
Transverse temporal gyrus	41, 42	1.6/2.1	34.9 (–50, –17,12)/32.0 (50, –20, 12)
Precentral gyrus	6, 13, 44, 43, 3, 9	13.2/ 11.7	34.8 (–48, –8, 6)/34.1 (48, –11, 6)
Postcentral gyrus	43, 40, 3, 1, 2	9.6/9.9	29.6 (–48, –17, 15)/28.4 (53, –20, 15)
Component 17			
Inferior parietal lobule	40, 7, 39	15.8/15.7	35.3 (–45, –41, 49)/36.6 (42, –44, 49)
Subgyral	40, 6, 7, 37, 10	5.6/12.6	22.8 (–36, –39, 43)/31.9 (36, –41, 46)
Postcentral gyrus	40, 5, 2, 3, 7, 1	6.5/14.0	26.9 (–48, –33, 49)/29.5 (48, –33, 49)
Superior parietal lobule	7, 5	6.7/6.8	27.5 (–36, –56, 50)/28.7 (36, –53, 52)
Precuneus	7, 19, 39	7.3/12.0	26.0 (–36, –65, 42)/24.4 (27, –56, 50)
Component 19			
Inferior parietal lobule	40	5.5/5.6	18.8 (–62, –31, 26)/18.6 (56, –34, 27)
Postcentral gyrus	7, 5, 40, 2, 1, 3, 43	5.4/3.5	24.0 (–6, –49, 63)/26.6 (6, –49, 63)
Superior temporal gyrus	22, 38, 42, 13, 39	5.0/5.2	23.2 (–53, 11, –6)/23.2 (45, 11, –6)
Insula	13, 47	4.8/5.5	23.9 (–42, 11, –3)/22.6 (45, 9, –3)
Paracentral lobule	5, 3, 7, 4, 31, 6	4.8/3.1	27.2 (–3, –44, 55)/27.0 (3, –44, 55)
Component 22			
Precuneus	31, 7, 39, 19, 23	27.3/25.3	46.9 (–6, –57, 30)/41.0 (3, –48, 33)
Cingulate gyrus	31, 24, 23	14.6/12.6	44.8 (–6, –45, 33)/42.8 (3, –45, 35)
Posterior cingulate	23, 31, 30, 29	3.7/4.4	40.2 (–6, –48, 25)/37.3 (6, –54, 25)
Cuneus	7, 19, 18	3.0/2.9	40.1 (–3, –65, 31)/36.9 (3, –65, 31)
Subgyral		6.1/4.4	30.3 (–12, –51, 25)/21.2 (15, –54, 25)
Component 23			
Posterior cingulate	30, 23, 29, 31, 18	6.5/9.1	37.7 (–6, –55, 17)/45.8 (6, –55, 11)
Precuneus	23, 31, 7, 19, 39	7.7/8.2	37.3 (–6, –60, 20)/41.0 (9, –60, 20)
Parahippocampal gyrus, hippocampus, amygdala	30, 36, 19, 37, 35, 27, 28, 34, 20	10.7/9.9	35.6 (–12, –49, 5)/32.5 (9, –46, 5)
Cuneus	30, 18, 7, 23, 17	2.8/4.2	25.7 (–9, –58, 6)/32.4 (9, –61, 9)
Culmen		4.1/4.5	28.3 (–9, –49, 2)/32.0 (9, –49, 2)
Component 25			
Posterior cingulate	30, 31, 23, 18, 29	5 1/4.5	41.3 (–6, –69, 12)/34.5 (12, –66, 12)
Cuneus	30, 23, 18, 17, 19, 7	21.3/ 21.4	39.8 (–6, –67, 9)/41.2 (3, –72, 9)

Table 4. Continued

Component 1—Talairach Regions	Brodmann Areas	R/L (cm^3)	Maximum *t* Values (R/L)
Lingual gyrus	18, 17, 19	13.4/12.9	37.4 (–6, –73, 4)/38.6 (6, –70, 3)
Precuneus	31, 7, 19, 23	9.6/6.4	33.4 (–6, –69, 20)/27.5 (3, –74, 29)
Subgyral		6.5/2.0	27.7 (–18, –69, 23)/17.2 (24, –67, –2)

Note: A Talairach labeling system was used to determine regions of significance at a threshold of ($P < 1.0 \times 10^{-10}$, false discovery rate).

in between bilateral anterior and posterior middle temporal gyri. Common regions of activation for C8 and C13 show a stronger overlap in the middle temporal gyrus, while the overlap for C3 and C13 can be found in superior temporal regions. Regions unique to each component were seen in prefrontal areas and posterior temporal gyri for C3, inferior frontal and parahippocampal gyrus for C8, and cerebellar and anterior temporal gyris for C13. We found that C13 exhibited the strongest positive activation across all components

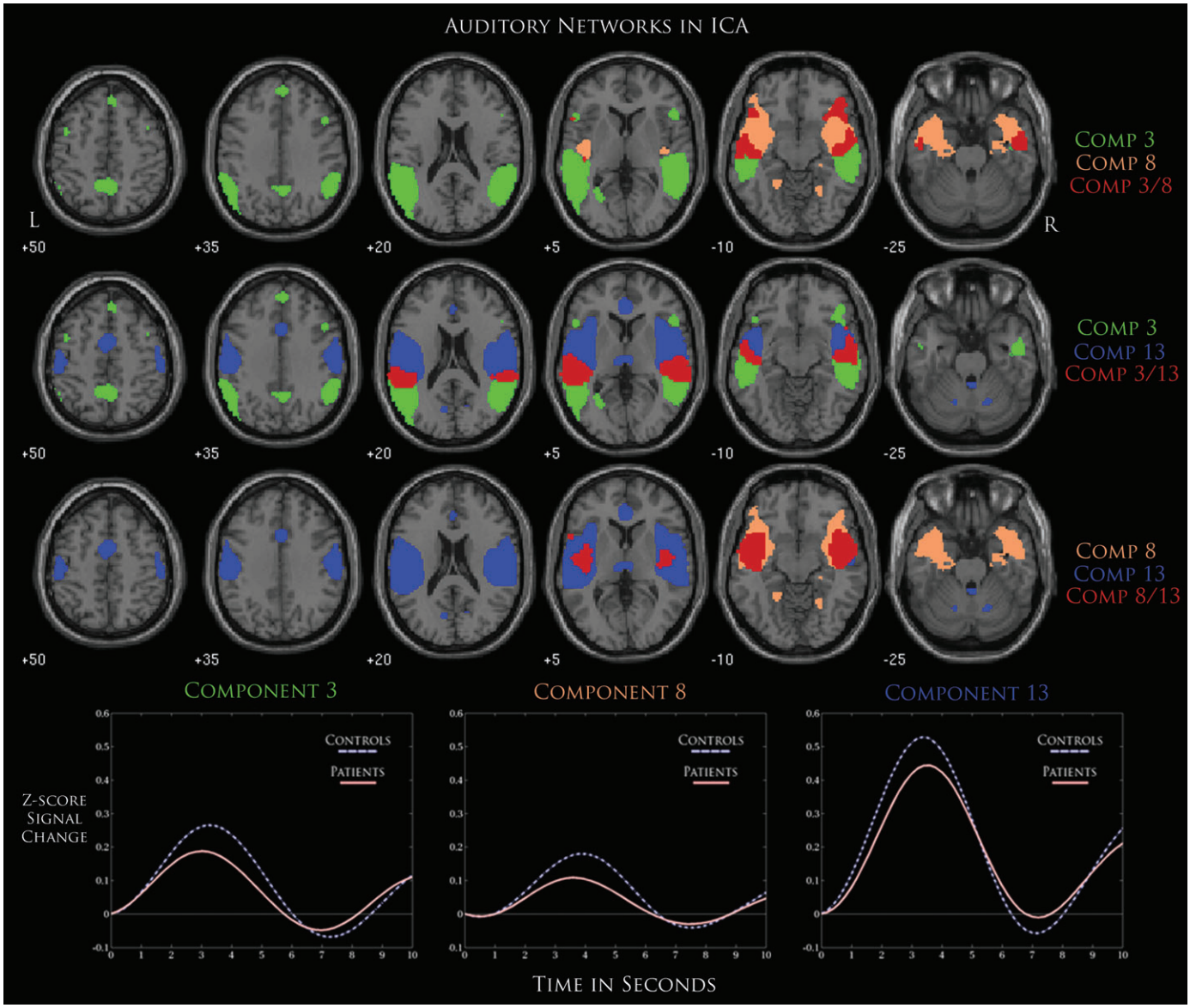

Fig. 4. An Overlay of 3 Components That Represent Possibly Auditory Networks (C3, C8, and C13) Thresholded at False Discovery Rate $P < 1.0 \times 10^{-10}$. Areas in red represent an overlap between 2 components where each row represents a distinctive pair of networks. Event-related averages for each component are also shown below with separate timecourses for patients and controls.

and found activation in regions such as the superior and transverse temporal gyri, which suggests that this component might be strongly linked to primary auditory regions. Similar to previous patterns of hypoactivity in patients, these 3 components showed a stronger positive modulation of the ICA timecourse in controls during the onset of the deviant stimulus.

We also found a component that represented the DMN in C22 and C23, where both networks shared activation in the posterior cingulate along with regions within the precuneus/cuneus. Only C22 was shown to exhibit significant between-group differences, but considering the similarities between their respective spatial maps we were again interested in comparing these 2 networks (figure 5). Concerning brain regions of activation, these 2 networks differed in that C23 showed activation in the parahippocampus, middle frontal gyrus, and cerebellum, while C22 uniquely showed activation in the thalamus while displaying more robust activation in the regions surrounding the posterior cingulate and precuneus. Significant overlap of activation was seen in the posterior cingulate and precuneus/cuneus regions along with a small area of the medial frontal gyrus. The event-related averages for C22 show a similar level of deactivation for controls and patients but with a significant delay for patients. Interestingly, the positive modulation of this timecourse differs drastically for controls and patients, where controls begin to return to baseline when $t = 3$, while this does not occur until $t = 5$ for patients.

Discussion

Using ICA, we identified multiple functionally connected networks involved in auditory target detection. Furthermore, we showed significant differences in schizophrenia patients in many of the networks that include regions commonly implicated in the illness, such as the bilateral temporal lobes, default-mode regions, and DLPFC. Noticeable decreases in the positive modulation of the ICA timecourses in patients suggest decreased brain activity relative to controls during auditory target detection, which might be further linked to the aberrant activity we found in the DMN. Abnormalities in multiple networks in schizophrenia suggest that the level of cognitive dysfunction is diffuse and widespread. This provides further support of theories suggesting that aberrant brain connectivity is a significant biological marker of the pathophysiology of schizophrenia.[11,24,31–33]

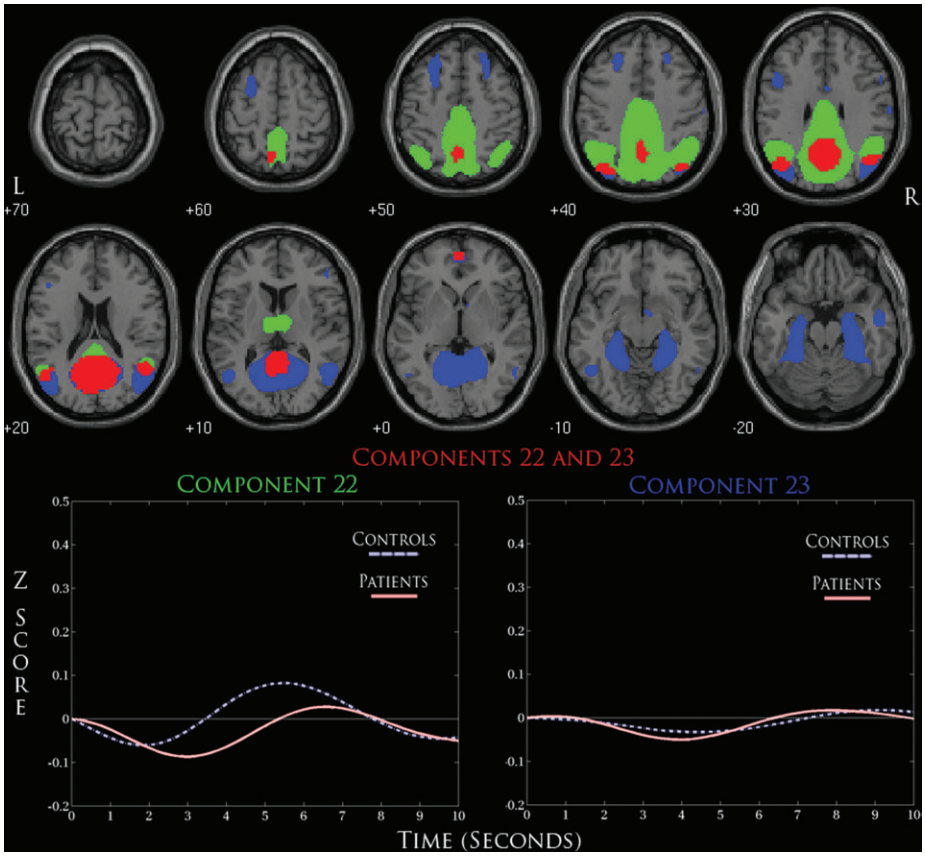

Fig. 5. A Detailed Overlay of Default-Mode Networks (C22 and C23) Thresholded at False Discovery Rate $P < 1.0 \times 10^{-10}$. Red areas represent overlapping regions of activation for both components. Event-related averages below for each component show a negatively modulated ICA timecourse.

Consistent with our hypothesis, we found deficits in auditory networks in patients with schizophrenia, similar to those seen by others,[9,34] including bilateral temporal lobes, anterior cingulate, and cerebellum. From our results, C3 and C8 characterized a bilateral temporal network containing regions such as the superior temporal and middle temporal gyri while also revealing significant between-group differences between patients and controls. However, we also considered C13 to be a component of interest because it uniquely depicted activation within the transverse temporal gyrus, a region synonymous with the primary auditory cortex, which suggested that this component was possibly engaged in the first-level processing of the auditory task stimulus.[35] Although ICA does not allow us to directly address this, a hierarchical relationship could exist where C13 represents a network that modulates the activation of C3 and C8. A recent study using diffusion tensor imaging (DTI) and Granger causality mapping (GCM) found structural and effective connectivity interactions between posterior and anterior STG during a simple sentence comprehension.[36] The overlapping regions for C3 and C8 also follow a similar relationship, where C3 shows a stronger posterior STG overlap and C8 exhibiting a more anterior STG localization. These common areas of activation suggest that one of the possible deficits in schizophrenia might occur during the transition from these primary regions to higher level associative regions. Deficits in the maintenance of selective attention during ERP recordings of a similar paradigm support this idea and suggest a possible aberrant connectivity between these frontal-temporal regions.[37]

A large number of studies have recently focused on the DMN and its relation to other regions within the brain. This network is a hypothesized conglomeration of regions that are recruited during a baseline state of activity when the participant is not engaged in any goal-directed behavior.[38] A recent study by Garrity et al,[11] using ICA on a similar auditory oddball paradigm, showed that patients with schizophrenia exhibit aberrant connectivity within this particular network, which consists of regions such as the posterior cingulate, precuneus, cingulate gyrus, and cuneus. Using the same analysis methods on a slightly modified oddball paradigm, we found that our results from C22 replicate that previous study. The event-related average for this component shows that patients tend to remain longer than controls in a negatively modulated state followed by a significantly weaker positive modulation. This might suggest that schizophrenia patients have difficulty shifting away from their baseline activity and modulating other networks accordingly to the task at hand. Our overlay of this component with C23 is an attempt at further exploring the interesting similarities and dynamics seen in both networks through ICA and to suggest that the regions normally associated with the DMN could be represented as multiple networks, also stated by Buckner et al.[14] In a similar vein to the auditory networks mentioned above, the stronger modulation of C22 could represent a primary baseline network that is further dissociated into other DMN regions as a secondary system. The strong overlap between the posterior cingulate, precuneus/cuneus, and anterior cingulate regions for both components and their negative modulated timecourses suggest a possible functional relationship between them, which our current analysis cannot confirm. However, there are established methods that determine temporal correlations[24] and causal relationships[39] between these independent components and future studies that probe this relationship could further strengthen this hypothesis.

There were multiple networks involving prefrontal regions such as C6, C17, and C19, including DLPFC, a region known to be involved in working memory.[40] This regions is also found to be consistently dysfunctional in schizophrenia[41,42] and their unaffected first-degree relatives, suggesting a genetic basis for DLPFC dysfunction.[43] The event-related averages for these 3 networks show that patients are exhibiting a level of hypofrontality supported by previous fMRI studies of schizophrenia.[44–46] As for C17, there seems to be a large difference not only in the amplitude of the timecourse but also in its shape where patients show an almost absent modulation of the timecourse. A similar component was seen in a previous resting-state analysis of fMRI subjects using ICA and was initially proposed as representative of a dorsal visual stream network.[12] If so, this would provide further support to studies that have shown sensory deficits in schizophrenia affecting dorsal visual pathways within the brain.[47,48]

Involvement of these anatomical areas in target detection tasks, as well as their reductions in schizophrenia, is consistent with the large P300 literature showing P300 amplitude reductions in the illness.[49,50] Like the activations associated with target detections, P300 is generated in widespread cortical areas of the lateral prefrontal cortex, temporoparietal junction, and parietal lobes.[51] The similarity of these findings across different modalities (fMRI and ERP) suggest that these areas might represent a consistent biological marker in the characterization of schizophrenia.

It is important to stress that the independent cognitive systems found using ICA are not necessarily unique for every analysis. For our purposes, C1, C6, C17, and C25 can be considered components that have been represented in a previous resting-state connectivity study using ICA.[12,13,52] C1 exhibited strong robust activation within the cerebellum and has been found in previous ICA analyses of auditory oddball experiments and resting-state analyses.[53] Differences within this network also support previous studies that show dysfunction in cerebellar regions for schizophrenia as well as providing some support to the cortico-cerebellar-thalamic-circuitry dysruption theorized by Andreasen et al.[54] In C6, the activation of superior

and middle frontal gyri along with the anterior cingulate have suggested that this network might represent an executive control system that engages in overriding other regions of the brain to implement cognitive control.[55] For C25, activation in the medial visual cortical areas suggests that this network might engage primary visual areas that are further linked to the thalamus for further visual processing.[56] A recent study by Calhoun et al[53] using ICA showed a similar component in both an auditory oddball task and a resting-state task along with group differences between schizophrenia patients and controls. This highlights one of the advantages of using a method such as ICA, which can extract signals that represent possible functional networks, which could then turn out to be highly task related. Examination of how these systems are modulated might yield the greatest insight into the biologically consistent features of schizophrenia and the cognitive deficits that often accompany them.

Although the availability of a larger subject sample size for fMRI analysis (assuming the task is well controlled and the subjects carefully chosen) leads to a more powerful test of a given hypothesis, the cognitive heterogeneity of schizophrenia suggests that biomarkers relevant to this disorder might be obscured due to group averaging.[57]The fact that this analysis was a conglomeration of multiple datasets across different sites adds to the concern of heterogeneity, and we attempted to account for this effect by including site as a covariate in our regression models. There are also certain limitations to ICA that must be considered. Though it gains certain advantages from being a data-driven algorithm, it is limited by the constraint that these functional networks are considered a linear mixture of independent signals. In this regard, nonlinear approaches to ICA might find very different networks that are indicative of meaningful brain activity. Also, functional connectivity differences in a general ICA analyses are limited to the differences found in the modulation of the ICA timecourse, and thus, the exact nature of this difference, (ie, whether a specific region within the network is responsible for these differences) cannot be determined unless higher order analyses such as effective connectivity measures are performed.[7,58–60]

The medication history of patients with schizophrenia was not accounted for during the fBIRN study. Patients were considered to be evaluated with chronic schizophrenia and stabilized with medication by a medically licensed physician. However, a detailed history of medications would provide the possibility for interesting correlational analyses with the results from ICA as well as accounting for possible confounds caused by these medications. It would also allow us to determine if particular psychotropics used by certain patients had a significant affect on the results of our ICA analysis. The effects of psychotropics on cognitive activity are often hard to assess, but they all have in common the ability to block D2 receptors. However, these medications differ in the potency of this blockade and vary in the types of receptors that are affected. Thus, a medication that is highly muscarinic may have some cognitive slowing and could present a potential confound in our analysis. Another possible limitation of our study can be in our decision to group schizoaffective patients with schizophrenia patients. If there are strong neurobiological differences in the pathology of one versus the other, it could then represent a potential confound in our analysis.

The elucidation of cognitive deficits in schizophrenia has been an important step toward parsing the neurocognitive pathology of this highly complex disorder. The analysis of these deficits in neuroimaging studies can benefit from the application of various signal-processing techniques. Using ICA, we were able to identify functionally independent networks that coincide with regions previously associated with the auditory oddball paradigm. We identified multiple networks that are implicated in schizophrenia that might play a significant role in the characterization of this disorder. We found a strong concentration of networks that lie within the DLPFC regions along with bilateral temporal lobes. Our results also showed that the DMN was implicated in schizophrenia, confirming previous studies that have found similar results using ICA. Future studies could benefit from a focus on the interaction of these networks and their distinction from one another, which could further elucidate important cognitive characteristics associated with schizophrenia. The benefits of our approach are in the large-scale analysis of multiple subjects using an approach that is able to identify deficits in functionally connected networks that are not contingent on a predefined hemodynamic response. Our findings support and extend the numerous studies that have identified similar regions associated with cognitive deficits in patients with schizophrenia.

Funding

National Institutes of Health (1 R01 EB #000840); NCRR (U24-RR021992).

Acknowledgments

Authorship contributions: Kim and Calhoun performed the data analyses and interpretation and wrote the manuscript; Mathalon, Ford, and Turner helped design and implement the experiment and provided editorial comments on the analyses and interpretation; the remaining authors designed and implemented the experiment, collected the data, and facilitated the imaging and behavioral data sharing to make these analyses possible. The inclusion of the fBIRN as an author represents the efforts of many otherwise unlisted researchers over the years who also had explicit input into the conception, design, and implementation of the work.

Appendix

Fig. A1.

References

1. Jeon YW, Polich J. Meta-analysis of P300 and schizophrenia: patients, paradigms, and practical implications. *Psychophysiology*. 2003;40:684–701.
2. Halgren E, Marinkovic K, Chauvel P. Generators of the late cognitive potentials in auditory and visual oddball tasks. *Electroencephalogr Clin Neurophysiol*. 1998;106:156–164.
3. McCarthy G, Wood CC. Intracranial recordings of endogenous ERPs in humans. *Electroencephalogr Clin Neurophysiol Suppl*. 1987;39:331–337.
4. Ross CA, Margolis RL, Reading SA, Pletnikov M, Coyle JT. Neurobiology of schizophrenia. *Neuron*. 2006;52:139–153.
5. Friston KJ. The disconnection hypothesis. *Schizophr Res*. 1998;30:115–125.
6. Lawrie SM, Buechel C, Whalley HC, Frith CD, Friston KJ, Johnstone EC. Reduced frontotemporal functional connectivity in schizophrenia associated with auditory hallucinations. *Biol Psychiatry*. 2002;51:1008–1011.
7. Kim D, Burge J, Lane T, Pearlson GD, Kiehl KA, Calhoun VD. Hybrid ICA-Bayesian network approach reveals distinct effective connectivity differences in schizophrenia. *NeuroImage*. 2008;42(4):1560–1568.
8. Calhoun VD, Adali T, Pearlson GD, Pekar JJ. Spatial and temporal independent component analysis of functional MRI data containing a pair of task-related waveforms. *Hum Brain Mapp*. 2001;13:43–53.
9. Kiehl KA, Stevens MC, Celone K, Kurtz M, Krystal JH. Abnormal hemodynamics in schizophrenia during an auditory oddball task. *Biol Psychiatry*. 2005;57:1029–1040.
10. Calhoun VD, Adali T, Giuliani NR, Pekar JJ, Kiehl KA, Pearlson GD. Method for multimodal analysis of independent source differences in schizophrenia: combining gray matter structural and auditory oddball functional data. *Hum Brain Mapp*. 2006;27:47–62.
11. Garrity AG, Pearlson GD, McKiernan K, Lloyd D, Kiehl KA, Calhoun VD. Aberrant "default mode" functional connectivity in schizophrenia. *Am J Psychiatry*. 2007;164:450–457.
12. Beckmann CF, De Luca M, Devlin JT, Smith SM. Investigations into resting-state connectivity using independent component analysis. *Philos Trans R Soc Lond B Biol Sci*. 2005;360:1001–1013.
13. Damoiseaux JS, Rombouts SA, Barkhof F, et al. Consistent resting-state networks across healthy subjects. *Proc Natl Acad Sci USA*. 2006;103:13848–13853.
14. Buckner RL, Andrews-Hanna JR, Schacter DL. The brain's default network: anatomy, function, and relevance to disease. *Ann N Y Acad Sci*. 2008;1124:1–38.
15. Friedman L, Stern H, Brown GG, et al. Test-retest and between-site reliability in a multicenter fMRI study. *Hum Brain Mapp*. 2008;29(8):958–972.
16. Andreasen NC, ed. *Scale for the Assessment of Positive Symptoms (SAPS)*. Iowa City, Iowa: University of Iowa; 1984.
17. Andreasen NC, ed. *Scale for the Assessment of Negative Symptoms (SANS)*. Iowa City, Iowa: University of Iowa; 1983.
18. Friedman L, Magnotta V, Posse S. FIRST BIRN (2004) scanner differences in the smoothness of fMRI images: implications for multi-center studies. *Proc ISMRM*. 2004;1074.
19. Freire L, Mangin JF. Motion correction algorithms may create spurious brain activations in the absence of subject motion. *NeuroImage*. 2001;14:709–722.
20. Freire L, Roche A, Mangin JF. What is the best similarity measure for motion correction in fMRI time series? *IEEE Trans Med Imaging*. 2002;21:470–484.
21. Ashburner J, Friston KJ. Nonlinear spatial normalization using basis functions. *Hum Brain Mapp*. 1999;7:254–266.
22. Calhoun VD, Adali T, Pearlson GD, Pekar JJ. A method for making group inferences from functional MRI data using independent component analysis. *Hum Brain Mapp*. 2001;14:140–151.
23. Stevens MC, Kiehl KA, Pearlson G, Calhoun VD. Functional neural circuits for mental timekeeping. *Hum Brain Mapp*. 2007;28:394–408.
24. Jafri MJ, Pearlson GD, Stevens M, Calhoun VD. A method for functional network connectivity among spatially independent resting-state components in schizophrenia. *NeuroImage*. 2008;39:1666–1681.
25. Li YO, Adali T, Calhoun VD. Estimating the number of independent components for functional magnetic resonance imaging data. *Hum Brain Mapp*. 2007;28:1251–1266.
26. Stevens M, Kiehl KA, Pearlson GD, Calhoun VD. Functional neural circuits for mental timekeeping. *Hum Brain Mapp*. 2007;28(5):394–408.
27. Bell AJ, Sejnowski TJ. An information maximisation approach to blind separation and blind deconvolution. *Neural Comput*. 1995;7:1129–1159.
28. Beckmann CF, DeLuca M, Devlin JT, Smith SM. Investigations into resting-state connectivity using independent component analysis. *Philos Trans R Soc Lond*. 2005;360:1001–1013.
29. Genovese CR, Lazar NA, Nichols T. Thresholding of statistical maps in functional neuroimaging using the false discovery rate. *Neuroimage*. 2002;15:870–878.
30. Calhoun VD, Kiehl KA, Liddle PF, Pearlson GD. Aberrant localization of synchronous hemodynamic activity in auditory cortex reliably characterizes schizophrenia. *Biol Psychiatry*. 2004;55:842–849.
31. Friston KJ, Frith CD. Schizophrenia: a disconnection syndrome? *Clin Neurosci*. 1995;3:89–97.

32. Honey GD, Pomarol-Clotet E, Corlett PR, et al. Functional dysconnectivity in schizophrenia associated with attentional modulation of motor function. *Brain*. 2005;128(pt 11): 2597–2611.
33. Schlosser R, Gesierich T, Kaufmann B, et al. Altered effective connectivity during working memory performance in schizophrenia: a study with fMRI and structural equation modeling. *Neuroimage*. 2003;19:751–763.
34. Laurens KR, Kiehl KA, Ngan ET, Liddle PF. Attention orienting dysfunction during salient novel stimulus processing in schizophrenia. *Schizophr Res*. 2005;75:159–171.
35. Palmer AR, Summerfield AQ. Microelectrode and neuroimaging studies of central auditory function. *Br Med Bull*. 2002;63:95–105.
36. Upadhyay J, Silver A, Knaus TA, et al. Effective and structural connectivity in the human auditory cortex. *J Neurosci*. 2008;28:3341–3349.
37. Mathalon DH, Heinks T, Ford JM. Selective attention in schizophrenia: sparing and loss of executive control. *Am J Psychiatry*. 2004;161:872–881.
38. Raichle ME, MacLeod AM, Snyder AZ, Powers WJ, Gusnard DA, Shulman GL. A default mode of brain function. *Proc Natl Acad Sci USA*. 2001;98:676–682.
39. Londei A, D'Ausilio A, Basso D, et al. Brain network for passive word listening as evaluated with ICA and Granger causality. *Brain Res Bull*. 2007;72:284–292.
40. Goldman-Rakic PS. Cellular basis of working memory. *Neuron*. 1995;14:477–485.
41. Goldman-Rakic PS. Working memory dysfunction in schizophrenia. *J Neuropsychiatr Clin Neurosci*. 1994;6:348–357.
42. Honey GD, Fletcher PC. Investigating principles of human brain function underlying working memory: what insights from schizophrenia? *Neuroscience*. 2006;139:59–71.
43. Park S, Holzman PS, Goldman-Rakic PS. Spatial working memory deficits in the relatives of schizophrenic patients. *Arch General Psychiatry*. 1995;52:821–828.
44. Weinberger DR, Berman KF, Zec RF. Physiologic dysfunction of dorsolateral prefrontal cortex in schizophrenia. I. Regional cerebral blood flow evidence. *Arch Gen Psychiatry*. 1986;43:114–124.
45. Andreasen NC, Rezai K, Alliger R, et al. Hypofrontality in neuroleptic-naive patients and in patients with chronic schizophrenia. Assessment with xenon 133 single- photon emission computed tomography and the Tower of London. *Arch Gen Psychiatry*. 1992;49:943–958.
46. Barch DM, Carter CS, Braver TS, et al. Selective deficits in prefrontal cortex function in medication-naive patients with schizophrenia. *Arch Gen Psychiatry*. 2001;58:280–288.
47. Doniger GM, Foxe JJ, Murray MM, Higgins BA, Javitt DC. Impaired visual object recognition and dorsal/ventral stream interaction in schizophrenia. *Arch Gen Psychiatry*. 2002;59: 1011–1020.
48. O'Donnell BF, Swearer JM, Smith LT, Nestor PG, Shenton ME, McCarley RW. Selective deficits in visual perception and recognition in schizophrenia. *Am J Psychiatry*. 1996;153:687–692.
49. Ford JM, White P, Lim KO, Pfefferbaum A. Schizophrenics have fewer and smaller P300s: a single-trial analysis. *Biol Psychiatry*. 1994;352:96–103.
50. Ford JM. Schizophrenia: the broken P300 and beyond. *Psychophysiology*. 1999;36:667–682.
51. Soltani M, Knight RT. Neural origins of the P300. *Crit Rev Neurobiol*. 2000;14:199–224.
52. De Luca M, Beckmann CF, De Stefano N, Matthews PM, Smith SM. fMRI resting state networks define distinct modes of long-distance interactions in the human brain. *NeuroImage*. 2006;29:1359–1367.
53. Calhoun VD, Kiehl KA, Pearlson GD. Modulation of temporally coherent brain networks estimated using ICA at rest and during cognitive tasks. *Hum Brain Mapp*. 2008;29(7):828–838.
54. Andreasen NC, Paradiso S, O'Leary DS. "Cognitive dysmetria" as an integrative theory of schizophrenia: a dysfunction in cortical-subcortical-cerebellar circuitry? *Schizophr Bull*. 1998;24:203–218.
55. Miller EK, Cohen JD. An integrative theory of prefrontal cortex function. *Annu Rev Neurosci*. 2001;24:167–202.
56. Behrens TE, Johansen-Berg H, Woolrich MW, et al. Non-invasive mapping of connections between human thalamus and cortex using diffusion imaging. *Nat Neurosci*. 2003;6:750–757.
57. Manoach DS. Prefrontal cortex dysfunction during working memory performance in schizophrenia: reconciling discrepant findings. *Schizophr Res*. 2003;60:285–298.
58. Friston KJ, Harrison L, Penny W. Dynamic causal modelling. *NeuroImage*. 2003;19:1273–1302.
59. Petersson KM, Nichols TE, Poline JB, Holmes AP. Statistical limitations in functional neuroimaging. I. Non-inferential methods and statistical models. *Philos Trans R Soc Lond B Biol Sci*. 1999;354:1239–1260.
60. Petersson KM, Nichols TE, Poline JB, Holmes AP. Statistical limitations in functional neuroimaging. II. Signal detection and statistical inference. *Philos Trans R Soc Lond B Biol Sci*. 1999;354:1261–1281.